Olefin/ Paraffin Separations by Adsorption: π-Complexation vs. Kinetic Separation

Salil U. Rege, Joel Padin, and Ralph T. Yang
Dept. of Chemical Engineering, University of Michigan, Ann Arbor, MI 48109

Monolayer dispersed $AgNO_3$ on silica gel was prepared by thermal dispersion. This sorbent exhibited superior adsorption properties for olefin/paraffin separations by selective adsorption of olefins through π-complexation. This sorbent, along with Ag^+ ion-exchanged resin, was subjected to simulation studies for olefin/paraffin separations by pressure-swing adsorption. Kinetic separations (due to differences in olefin/paraffin diffusivities) using zeolite 4A and molecular-sieve carbon were also studied. Using 50/50 mixtures of C_2H_4/C_2H_6 and C_3H_6/C_3H_8, separations using these sorbents were compared directly based on olefin product purity, recovery, and throughput. The monolayer $AgNO_3/SiO_2$ sorbent showed superior separation results for C_3H_6/C_3H_8, and the Ag^+-exchanged resin showed best results for C_2H_4/C_2H_6. In both cases, over 99% product purities could be obtained at reasonably high recoveries and throughputs. For C_3H_6/C_3H_8 separation on $AgNO_3/SiO_2$, multiplicity of cyclic steady states were observed within certain regions of feed and purge velocities. Within these regions, two stable cyclic steady states were reached starting from different initial-bed conditions while all operating conditions were identical.

Introduction

Olefin/paraffin separations represent a class of the most important and also the most costly separations in the chemical and petrochemical industry. Cryogenic distillation has been used for over 60 years for these separations (Keller et al., 1992). They remain the most energy-intensive distillations because of the close relative volatilities. For example, ethane/ethylene separation is carried out at about -25°C and 320 psig (2.306 MPa) in a column containing over 100 trays, and propane/propylene separation is performed by an equally energy-intensive distillation at about -30°C and 30 psig (0.308 MPa) (Keller et al., 1992). A number of alternatives have been investigated (Eldridge, 1993); the most promising one appears to be π-complexation.

Separation by π-complexation is a subgroup of chemical complexation where the mixture is contacted with the second phase, which contains a complexing agent (King, 1987). The advantage of chemical complexation is that the bonds formed are stronger than those by van der Waals forces alone, so it is possible to achieve high selectivity and high capacity for the component to be bound; at the same time, the bonds are still weak enough to be broken by using simple engineering operations such as raising the temperature or decreasing the pressure.

The π-complexation pertains to the main group (or d-block) transition metals, that is, from Sc to Cu, Y to Ag, and La to Au in the periodic table (Cotton and Wilkinson, 1966). These metals or their ions can form the normal σ bond to carbon and, in addition, the unique characteristics of the d orbitals in these metals or ions can form bonds with the unsaturated hydrocarbons (olefins) in a nonclassic manner. This type of bonding is broadly referred to as π-complexation, which has been seriously considered for olefin/paraffin separation and purification by employing liquid solutions containing silver (Ag^+) or cuprous (Cu^{+1}) ions (Quinn, 1971; Ho et al., 1988; Keller et al., 1992; Blytas, 1992; Eldridge, 1993). These involved gas/liquid operations. While gas/solid operations can be simpler as well as more efficient, particularly by pressure-swing adsorption, the list of attempts for developing solid π-complexation sorbents is a short one. CuCl in the form of crystals, which is insoluble in water, has been considered for olefin/paraffin separations (Gilliland et al., 1941; Gilliland, 1945; Long, 1972). Other attempts on solid sorbents for π-

Correspondence concerning this article should be addressed to R. T. Yang.

complexation include Ag salts supported on *anion* exchange resins (Hirai et al., 1985a,b), AgY zeolite (Yang and Kikkinides, 1995), and CuY zeolite (Cen, 1991). The only apparently successful solid sorbent of this nature was $CuCl/\gamma$-Al_2O_3 for binding with the π bond of CO (Xie and Tang, 1990; Kumar et al., 1993). It should also be noted that the commercially available sorbents do not have significant selectivities for olefins (over corresponding paraffins), and the use of these sorbents would require additional, substantial operations (Kulvaranon et al., 1990; Kumar et al., 1992; Jarvelin and Fair, 1993; Ghosh et al., 1993).

More recently, a number of new π-complexation sorbents were prepared for selective olefin adsorption. These include Ag^+-exchanged resins (Yang and Kikkinides, 1995; Wu et al., 1997), monolayer $CuCl/\gamma$-Al_2O_3 (Yang and Kikkinides, 1995), and monolayer CuCl on pillared clays (Cheng and Yang, 1995). For selective adsorption of acetylene from olefins and paraffins, monolayer Fe^{2+}, Co^{2+}, and Ni^{2+} salts on various substrates proved to be effective (Yang and Foldes, 1996; Padin and Yang, 1997). The π-complexation bonds are reasonably understood through molecular orbital studies (Chen and Yang, 1995; Chen and Yang, 1996). For C_3H_6/C_3H_8 separation, however, these sorbents do not provide a large working capacity for C_3H_6 since the C_3H_6 isotherms do not exhibit a steep portion between adsorption and desorption pressures. Hence the first goal of this work was to prepare a superior sorbent for selective C_3H_6 adsorption.

Separation can also be accomplished by differences in the diffusivities of different molecules from the mixture, known as kinetic separation (Yang, 1987). Indeed, there was a patent application disclosure indicating that 4A zeolite could be used for such separations (Ramachandran and Dao, 1995). In this work, the kinetic separations using 4A zeolite were studied and compared with equilibrium separations using π-complexation sorbents.

Multiplicity of periodic steady states remains a most intriguing aspect of cyclic adsorption processes (Croft and LeVan, 1994a,b). For pressure swing adsorption (PSA), it is possible that multiple steady states exist for a fixed set of operating conditions, over a particular range of one or more of these operating variables (i.e., bifurcation variables). The final stable state would depend only on the initial condition (i.e., the perturbation variables). Such an example of multiplicity in PSA has been presented by Kikkinides et al. (1995) for the system of $H_2S/CO_2/CH_4$ on 5A zeolite. Multiplicity is prevalent in reaction engineering, as described by Gavalas (1966), Luss and Amundson (1967), Aris (1969), Iooss and Joseph (1980), and Jensen and Ray (1982). Efficient methods for direct determination of periodic steady states as well as mapping regions with different bifurcation diagrams are available for reactor theory (Khinast and Luss, 1997), and should be applicable to PSA studies. In this study, we have identified a region of multiplicity for C_3H_6/C_3H_8 separation by PSA.

Experimental Section

Equilibrium isotherms, heats of adsorption, and temperature-dependent diffusivities were measured for four gases on three sorbents. Three sorbents were used in this study; two were commercial sorbents (4A zeolite and carbon molecular sieve) and one was a π-complexation sorbent prepared for this study ($AgNO_3/SiO_2$).

The 4A-type zeolite used was in powder form. The samples were degassed *in vacuo* (10^{-6} torr) at 350°C before each experiment. The carbon molecular sieve (CMS) utilized in this work was manufactured by Bergbau-Forschung GmbH in Germany. Unlike type-4A zeolite, which has a discrete pore size, Bergbau-Forschung CMS has a pore-size distribution between 3 and 5 Å. The sample utilized in this work was in pellet form. It was shown by Chen et al. (1994) that use of the pelletized form of CMS does not affect diffusion measurements, since diffusion processes in Bergbau-Forschung CMS are controlled by intracrystalline diffusion. The CMS samples were degassed *in vacuo* at 90°C before each experiment.

The π-complexation sorbent used in this work was prepared using thermal monolayer dispersion to disperse $AgNO_3$ over an SiO_2 substrate. The sorbent was prepared by mixing 0.32 g of $AgNO_3$ (Strem Chemicals) per gram of SiO_2 (Strem Chemicals). The SiO_2 had a surface area of 670 m^2/g and a pore volume of 0.46 cm^3/g. The particle size of the SiO_2 utilized ranged from 100 to 200 mesh. After thorough mixing, the sample was heated in air at 200°C for 89 h to assure complete dispersion. The BET surface area of the sorbent was measured at 384 m^2/g by nitrogen adsorption at 77 K. Pore size was calculated to be 23 Å using the BJH method described in detail by Barett et al. (1951). Other $AgNO_3/SiO_2$ ratios were also used; the ratio just given yielded the best results.

Equilibrium isotherms, uptake curves, and surface-area measurements were made utilizing a Micromeritics ASAP 2010 adsorption instrument and a Shimadzu TGA-50 thermogravimetric analyzer. The ASAP 2010 utilizes a volumetric system to obtain adsorption isotherms and uptake curves. All uptake curves were measured at a stepped pressure increment from 0 atm to 0.1 atm. Also, measurements were made at various temperatures to obtain isosteric heat of adsorption data and the temperature dependence of diffusivities. Surface-area measurements were carried out by nitrogen adsorption at 77 K. The hydrocarbons used were: ethane (CP grade, Matheson minimum purity 99.0%), ethylene (CP grade, Matheson minimum purity 99.5%), propane (CP grade, Matheson minimum purity 99.0%), propylene (CP grade, Matheson minimum purity 99.0%). The gases were used without further purification.

Description of the PSA cycle

A four-step PSA cycle similar to that used by Kikkinides et al. (1993) was used in all the cases in this study. The steps involved in each cycle were as follows: (1) pressurization with the feed gas (mixture of 50% olefin and 50% paraffin on molar basis); (2) high-pressure adsorption with feed gas, that is, feedstep; (3) high-pressure cocurrent purge with part of the olefin-rich product obtained in step (4); (4) countercurrent blowdown to a low pressure. All the steps were of equal time duration.

Figure 1 shows the PSA cycle used. As can be seen, a portion of the high-purity olefin from the countercurrent blowdown step was compressed to the feed pressure and used for rinsing the bed cocurrently in step 3. It was shown earlier

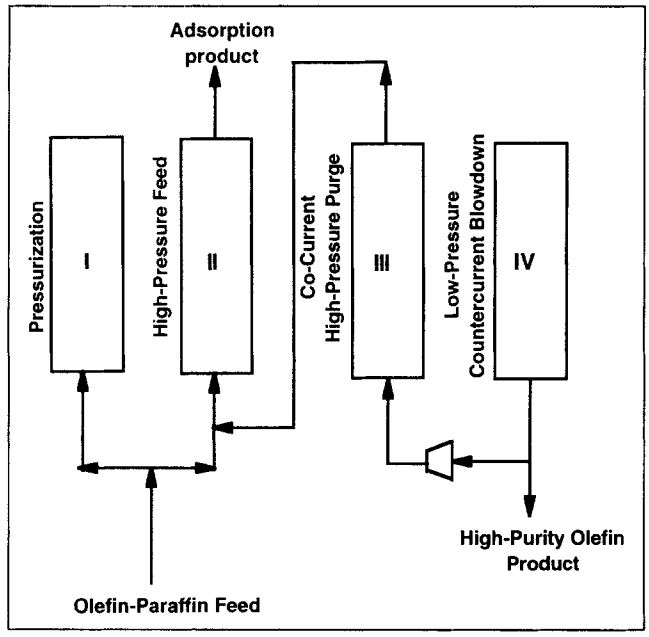

Figure 1. Sequence and basic steps in the four-step PSA cycle.

that purging with the strongly adsorbed component results in a significant increase in the purity of that component in the product stream (Sircar and Zondlo, 1977; Cen and Yang, 1986). In the present work, the product of the high-pressure rinse step is recycled and mixed volumetrically, with the feed gas supplied to step 2.

The objective of the present work was to compare the performance of adsorbents employing equilibrium separation, kinetic separation, and separation by exclusion of one of the components. This comparison needed to be carried out using nearly identical cycle conditions. In the case of ethane/ethylene separation, the adsorbents were compared at the same product throughput and the product purity was studied at various product recoveries. In the case of propane/propylene separation, the adsorbents had highly differing productivities, and hence the comparison was done at constant product purity and the product throughput was studied at various values of product recovery. It should be noted that the term "product" mentioned throughout this work refers to the olefin-rich product obtained in desorption step 4 unless otherwise specified. The various process variables used in this work were defined as follows:

Product recovery =

$$\frac{(C_3H_6 \text{ from step 4}) - (C_3H_6 \text{ used for purging in step 3})}{(C_3H_6 \text{ fed in step 1 and step 2})} \quad (1)$$

$$\text{Purge-to-feed ratio (P/F)} = \frac{(C_3H_6 \text{ used to purge in step 3})}{(C_3H_6 \text{ fed in step 1 and step 2})}. \quad (2)$$

Another important parameter used to gauge the adsorbent's productivity is the product throughput (also referred to as productivity in this work):

Product throughput

$$= \frac{\text{Amount (kg) of } C_3H_6 \text{ produced per hour}}{\text{Amount (kg) of adsorbent}}. \quad (3)$$

PSA simulation

The model used assumes the flow of a gaseous mixture of two components in an adiabatic fixed bed packed with spherical adsorbent particles of identical size and shape. Axial dispersion for mass and heat transfer is assumed, but dispersion in the radial direction is taken to be negligible. Axial pressure drop is neglected and ideal gas law is assumed to hold since pressures involved are low. External mass-transfer limitations are assumed to be negligible. Also the gas is assumed to have constant viscosity and heat capacity.

The mass-balance equation for component k in the bed is given by the axially dispersed plug flow equation (Sun et al., 1996):

$$\epsilon_t \frac{\partial y_k}{\partial t} - \epsilon D_{ax} \frac{\partial^2 y_k}{\partial z^2} + \epsilon \frac{\partial (u y_k)}{\partial z} + \frac{\rho_b RT}{P} \frac{\partial \overline{q_k}}{\partial t} + \frac{\epsilon_t y_k}{P} \frac{dP}{dt} = 0. \quad (4)$$

The overall material balance obtained is

$$\epsilon \frac{\partial u}{\partial z} = -\frac{\rho_b RT}{P} \sum_{k=1}^{2} \frac{\partial \overline{q_k}}{\partial t} - \frac{\epsilon_t}{P} \frac{dP}{dt}. \quad (5)$$

For an adiabatic bed with no heat transfer with the surroundings, the overall heat balance may be written as

$$\left[\epsilon \rho_g c_{pg} + \rho_b \left(c_{ps} + \sum_{k=1}^{2} \overline{q_k} c_{pg}\right)\right] \frac{\partial T}{\partial t} + \epsilon \rho_g c_{pg} u \frac{\partial T}{\partial z} - \epsilon \lambda_L \frac{\partial^2 T}{\partial z^2} = \rho_b \sum_{k=1}^{2} |\Delta H_j| \frac{\partial \overline{q_k}}{\partial t} + \epsilon \frac{dP}{dt}. \quad (6)$$

The axial dispersion coefficient (D_{ax}) and effective thermal conductivity (λ_L) were obtained from the mass and thermal Peclet numbers, respectively, which were obtained using standard correlations for dispersion in fixed beds (Yang, 1987).

The rate of uptake by a sorbent particle was assumed to follow the linear driving force (LDF) approximation, which holds true when $D_e t/R_p^2 > 0.1$:

$$\frac{\partial \overline{q_k}}{\partial t} = \frac{15 D_{e,k}}{R_p^2} (q_k^* - \bar{q}_k), \quad (7)$$

where q_k^* is the equilibrium amount adsorbed at the surface of the pellet. The LDF approximation was valid under the conditions used in this study.

Cross-term diffusivities were neglected. The effective diffusivity values ($D_{e,k}$) were assumed to be independent of the surface coverage, and they were assumed to have an exponential temperature dependence as follows:

$$D_{e,k} = D^0_{e,k} \exp\left[\frac{-E_{\text{act},k}}{R_g}\left(\frac{1}{T} - \frac{1}{T_{\text{ref}}}\right)\right], \tag{8}$$

where $D^0_{e,k}$ was the effective diffusivity at a reference temperature T_{ref}.

The initial conditions of each step were the conditions at the end of the preceding step. For the first step, the bed was maintained at 0.1 atm with a certain composition of the olefin/paraffin mixture. The pressurization and countercurrent blowdown steps were the only pressure-changing steps and the variation of pressure with time was assumed to be exponential:

$$P(t) = P_{\text{fin}} + (P_{\text{ini}} - P_{\text{fin}}) \exp(-t/t_s), \tag{9}$$

where t_s was a conveniently chosen time constant. The value of t_s has to be chosen sufficiently small so as to obtain the desired pressure change but also sufficiently large so as to keep the (dP/dt) term in the model small enough to avoid stiffness in the numerical method used. In general, t_s was 24–27% of the step time chosen.

The boundary conditions used were the Dankwerts' boundary conditions for the closed/closed vessel case:

$$D_{ax}\left.\frac{\partial y_k}{\partial z}\right|_{z=0} = u_m(y_k|_{z=0} - y_{H,k})$$

$$-\lambda_L\left.\frac{\partial T}{\partial z}\right|_{z=0} = \rho_g c_{pg} u_m(T|_{z=0} - T_H)$$

$$\left.\frac{\partial y_k}{\partial z}\right|_{z=L} = \left.\frac{\partial T}{\partial z}\right|_{z=L} = 0. \tag{10}$$

Here $z = 0$ and $z = L$ represent the entrance and exit points in the fixed bed, respectively. The subscript m refers to the number of the step in the cycle.

For adsorption by π-complexation, the equation giving the most satisfactory fit to experimental data has been known to be the Langmuir-uniform-distribution (LUD) equation (Yang and Kikkinides, 1995; Cheng and Yang, 1995). Both the physisorption and chemisorption terms were included in the isotherm. At present, however, no equation is available for its extension to multicomponent mixtures. Hence, the loading ratio correlation (LRC) extended to binary mixtures was used (Yang, 1987):

$$q^*_k = \frac{q_{m,k} b_k P^{n_k}}{1 + \sum_{j=1}^{2} b_j P^{n_j}}, \tag{11}$$

where q_m, b, and n were LRC parameters. The temperature dependence of q_m and b was given as

$$q_m = k_1 \exp(k_2/T); \qquad b = k_3 \exp(k_4/T). \tag{12}$$

The coupled partial differential equations were solved using an implicit finite difference scheme employing the Crank–Nicolson method (Carnahan et al., 1969). The fixed bed was discretized into 100 spatial points and time into 200 time steps. The details of the numerical scheme used are given elsewhere (Sun et al., 1996). The PSA code was written in FORTRAN and was executed using a SUN-SPARC workstation. The model and numerical method were found to be stable and convergent for all of the runs, and all mass balances were found to be valid within 4% relative error. The machine time required for computation of one PSA cycle was about 15–20 s, and cyclic steady state was reached in 200–500 cycles, depending upon the initial conditions used.

Results and Discussion

Isotherms and diffusivities on 4A zeolite

The pure-component equilibrium isotherms of C_2H_4 and C_2H_6 on 4A zeolite at 25°C and 70°C are shown in Figure 2. The equilibrium data were fitted well by the LRC model shown in Eq. 11. The fitting parameters are shown in Table 1. From Figure 2, the amounts adsorbed at 25°C and 1 atm for C_2H_4 and C_2H_6 were 2.8 and 2.4 mmol/g, respectively. Hence equilibrium separation would not be feasible.

Uptake rates were measured using Micromeritics ASAP 2010 at 25°C and 70°C, and the results are shown in Figure 3. The pressure increments were from 0 atm to 0.1 atm. At 25°C, after 15 s, C_2H_4 adsorption was approximately 75% complete, while C_2H_6 adsorption was only 15% complete. Diffusion time constants, D/R^2, were calculated by fitting experimental data with the solution of the diffusion equation for spherical particles (Kärger and Ruthven, 1992). The values of D/R^2 obtained for C_2H_4 and C_2H_6 at 25°C were 5.12×10^{-3} and 1.64×10^{-4}, L/s^{-1}, respectively. The ratio of these diffusivities was 31, which was similar to the ratio of pure-component diffusivities of O_2/N_2 in the commercial separation of air using a carbon molecular sieve. However, it was observed that the desorption rate of C_2H_4 on zeolite 4A was low compared to that of adsorption rate, thus giving it an irreversible nature. Unlike C_2H_4, C_2H_6 adsorption was completely reversible at this temperature.

For purpose of simulation, however, the adsorption and desorption rates were assumed to be equal. The results of the

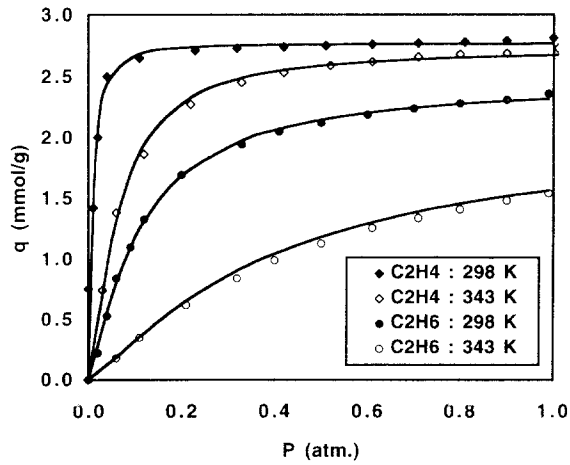

Figure 2. Equilibrium C_2H_4 and C_2H_6 isotherms on zeolite 4A at 25° and 70°C.

For all isotherm figures, symbols are experimental data and lines are fitted isotherms.

Table 1. Parameters in the Temperature-Dependent Loading Ratio Correlation Isotherms of C_2H_4, C_2H_6, C_3H_6 and C_3H_8 for Adsorbents

Sorbent	Sorbate	k_1 (mmol/g)	k_2 (K)	k_3 (atm^{-n})	k_4 (K)	n	$-\Delta H$ (kcal/mol)	C_{pg} (cal/mol/K)
Zeolite 4A	C_2H_4	2.462	3.529×10^{1}	1.38×10^{-6}	5,972	1.41	11.9	11.84
Zeolite 4A	C_2H_6	5.956×10^{-1}	4.232×10^{2}	9.00×10^{-5}	3,599	1.24	7.15	14.36
Zeolite 4A	C_3H_6	7.232×10^{-1}	3.449×10^{2}	2.81×10^{-5}	4,712	0.82	9.36	18.17
Zeolite 4A	C_3H_8	2.71	—	4.6×10^{-3}	—	0.46	—	21.30
Ag^+-resin	C_2H_4	2.94×10^{-2}	1.290×10^{3}	2.49×10^{-1}	632	0.67	9.35	11.84
Ag^+-resin	C_2H_6	4.53×10^{-4}	1.829×10^{3}	2.00×10^{-3}	0.0	2.17	4.6	14.36
CMS	C_2H_4	0.393	3.911×10^{2}	5.38×10^{-1}	568	0.98	3.25	11.84
CMS	C_2H_6	1.0×10^{-6}	3734	9×10^{-2}	200	0.5	—	14.36
$AgNO_3/SiO_2$	C_3H_6	1.09×10^{-1}	1.169×10^{3}	9.41×10^{-2}	811	0.68	11.5	18.17
$AgNO_3/SiO_2$	C_3H_8	4.09×10^{-1}	1.743×10^{3}	2.02×10^{-3}	270	0.69	3.35	21.30

simulation would thus represent the best separation of C_2H_4 and C_2H_6 by zeolite 4A at 25°C.

Equilibrium isotherms and diffusion time constants of C_3H_6 and C_3H_8 on 4A zeolite were also measured. The isotherms are shown in Figure 4, and the uptake rates of C_3H_6 are shown in Figure 5. It is noteworthy that C_3H_8 was essentially excluded from the 4A zeolite, whereas the C_3H_6 molecule was free to diffuse. The effective aperture size of the 4A zeolite is 3.8 Å, which obviously is the demarcation between the kinetic diameters of C_3H_6 and C_3H_8. The diffusion time constants of C_3H_6 at 25°C and 120°C were 8.5×10^{-5} L/s^{-1} and 4.3×10^{-4} L/s^{-1}, respectively. The temperature-dependent diffusivity values are included in Table 2. The equilibrium LRC fitting parameters are given in Table 1.

It was observed that the adsorption of C_3H_6 in the 4A zeolite was not completely reversible at 25°C, with approximately 10% adsorbate remaining after desorption. However, the adsorption at 120°C was readily reversible.

Isotherms and diffusivities on the carbon molecular sieve

Unlike the 4A zeolite with a discrete aperture dimension, the CMS had a distribution of micropore sizes ranging from 3 Å to 5 Å. Measurements with C_3H_6 and C_3H_8 showed that these molecules were totally excluded. The equilibrium isotherms of C_2H_4 and C_2H_6 at various temperatures are shown in Figure 6. C_2H_6 was nearly excluded, yet detectable amounts were observed due to the larger pores in the CMS. The diffusion time constants for C_2H_4 in CMS were 1.90×10^{-6} L/s^{-1} at 25°C and 1.77×10^{-5} L/s^{-1} at 100°C. The isotherm parameters are given in Table 1, and the temperature-de-pendent D/R^2 values are included in Table 2. Although the diffusivities were low, the equilibrium selectivity for C_2H_4/C_2H_6 was high. Hence the C_2/CMS system was included in PSA simulation.

Equilibrium isotherms and diffusivities on monolayer $AgNO_3/SiO_2$

Although both C_2H_4/C_2H_6 and C_3H_6/C_3H_8 separations appeared promising with the $AgNO_3/SiO_2$ π-complexation sorbent, only C_3H_6/C_3H_8 was included in this study. The Ag–resin was used for the C_2 separation for the purpose of evaluating separation by π-complexation. Data for C_2H_4 and C_2H_6 isotherms and diffusivity values were taken from the work by Wu et al. (1997) and are presented in Tables 1 and 2, respectively.

The equilibrum isotherms of C_3H_6 and C_3H_8 on $AgNO_3/SiO_2$ at 25°C and 70°C are shown in Figure 7. The Langmuir-type isotherm (i.e., LRC) did not fit the data well due to the steepness of the equilibrium data. The best fit is shown in Figure 7, and the fitting parameters are included in Table 1. Since the fitted isotherm undercalculated the Δq in the PSA cycle, the PSA simulation result based on the fitted isotherm would underestimate the separation.

The uptake rates were rapid and not shown here. For ex-

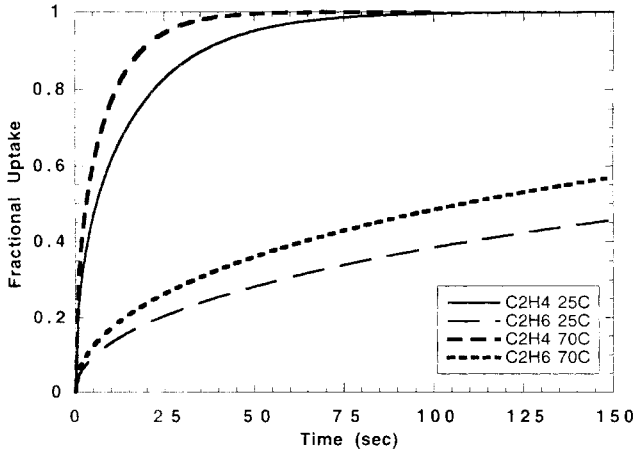

Figure 3. Uptake curves of C_2H_4 and C_2H_6 on zeolite 4A at 25° and 70°C at $P = 0$–0.1 atm.

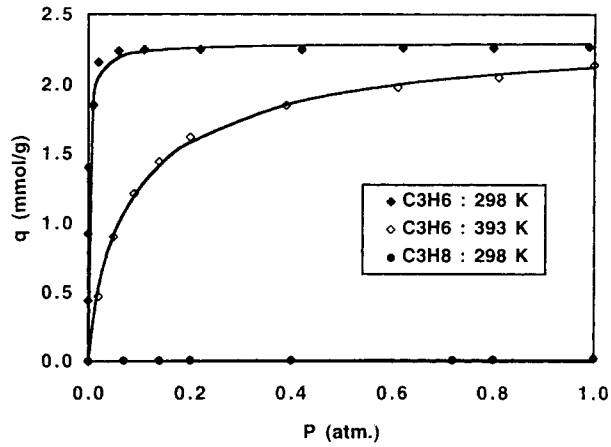

Figure 4. Equilibrium isotherms of C_3H_6 and C_3H_8 on zeolite 4A at 25° and 120°C.

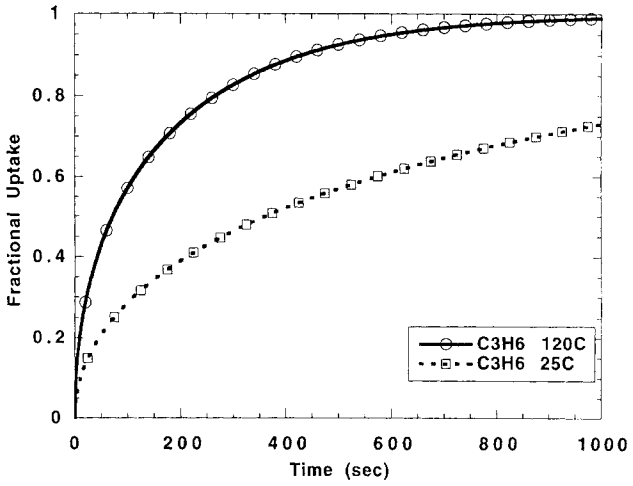

Figure 5. Uptake rates of C_3H_6 on zeolite 4A at 25° and 120°C.

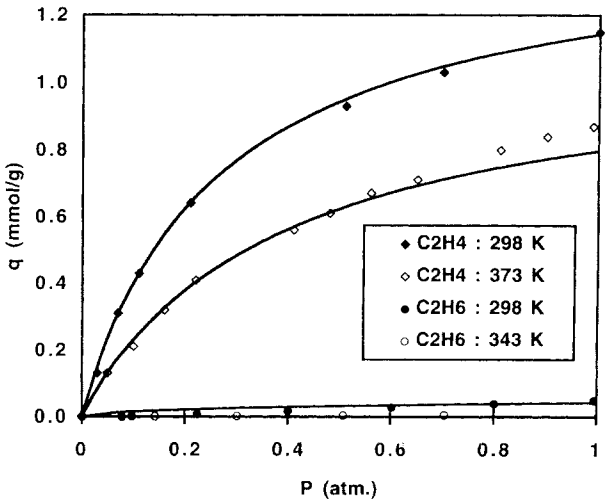

Figure 6. Equilibrium isotherms of C_2H_4 and C_2H_6 on molecular-sieve carbon at 25° and 100°C.

ample, the diffusion time constants for C_3H_6 and C_3H_8 at 70°C were 1.67×10^{-3} L/s^{-1} and 1.48×10^{-2} L/s^{-1}, respectively. The temperature-dependent values are included in Table 2. The rapid diffusion was due to the large pore dimensions (32 Å) in the sorbent.

Ethane/ethylene separation

The adsorbents that were considered for ethane/ethylene separation were zeolite 4A, Bergbau-Forschung carbon molecular sieve (CMS), and Ag^+-exchanged Amberlyst-35 resin. As discussed earlier, zeolite 4A had a good capacity for ethylene separation by way of kinetic separation, whereas the Bergbau-Forschung CMS had the property of excluding ethane completely. Recently, Ag^+-exchanged Amberlyst-35 with 36.5% degree of ion exchange (DIE) was found to have promising prospects for olefin/paraffin separation applications by virtue of steep isotherms for ethylene and comparatively flat isotherms for ethane (Wu et al., 1997).

The PSA cycle used is outlined in Table 3. In the case of zeolite 4A, a feed temperature of 25°C was used with time for each step ranging from 80 to 480 s. As was mentioned earlier, the desorption rate of C_2H_4 on zeolite 4A was low compared to that of adsorption at 25°C. In the present work, however, this irreversibility is neglected and equal rates of adsorption and desorption are assumed, thus giving the best separation possible by this sorbent. The purge-to-feed ratio was adjusted for each cycle time so as to provide an optimum product purity and recovery.

For Ag^+-exchanged resin, a feed temperature of 25°C was also employed for comparison with 4A zeolite. A study of the uptake curves for C_2H_4 provided by Wu et al. (1997) showed a 90% uptake after 30 min duration. Hence step times ranging from 800 s to 1,800 s were used.

The performance of the sorbents needed to be compared by keeping one of the following three parameters constant: product purity, product recovery, and product throughput. As comparable product throughputs were obtained in the case of zeolite 4A and the Ag^+–Amberlyst-35, comparison was done by studying the product purity vs. product recovery at an average product throughput of about 1.1×10^{-4} kg product/h/kg adsorbent. The PSA cycle conditions used in the

Table 2. Parameters Used in Calculating Temperature-Dependent Overall Diffusion Time Constant (D_e/R^2) for Diffusion of C_2H_4, C_2H_6, C_3H_6 and C_3H_8 in Adsorbents Used (Eq. 8)*

Sorbent	Sorbate	D_e^0/R^2 (s^{-1})	E_{act}/R_g (K)
Zeolite 4A	C_2H_4	5.12×10^{-3}	1,477
Zeolite 4A	C_2H_6	1.64×10^{-4}	1,231
Zeolite 4A	C_3H_6	8.49×10^{-5}	2,051
Zeolite 4A	C_3H_8	—	—
Ag^+–resin	C_2H_4	1.03×10^{-4}	766
Ag^+–resin	C_2H_6	1.07×10^{-4}	558
CMS	C_2H_4	1.89×10^{-6}	3,438
CMS	C_2H_6	—	—
$AgNO_3/SiO_2$	C_3H_6	1.43×10^{-3}	352
$AgNO_3/SiO_2$	C_3H_8	8.7×10^{-3}	1,206

*T_{ref} = 298 K.

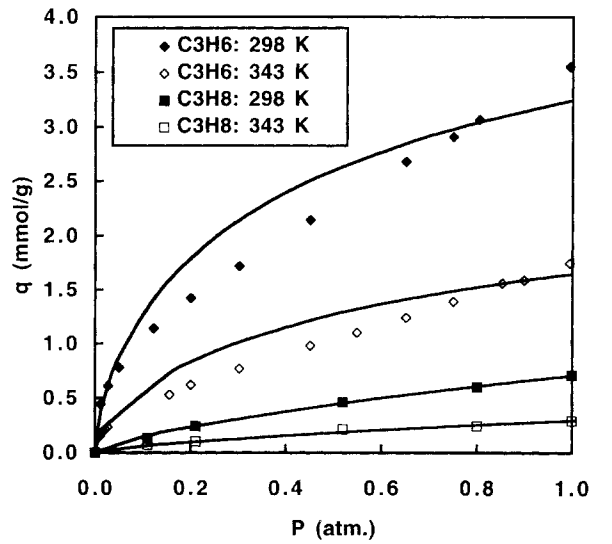

Figure 7. Equilibrium isotherms of C_3H_6 and C_3H_8 on monolayer $AgNO_3/SiO_2$ at 25° and 70°C.

Table 3. Adsorption Bed Characteristics and Operating Conditions Used in the PSA Simulations

Bed length	3.0 m
Diameter of adsorber bed	1.0 m
Bed external porosity	0.40
Bed density	720 kg/m^3
Heat capacity of bed	0.28 cal/g/K
Wall temperature	298 K (ambient)
Feed gas composition	50% olefin, 50% paraffin
Adsorption pressure (P_H)	1.0 bar
Desorption pressure (P_L)	0.1 bar
Initial total pressure	0.1 bar
Axial dispersion coefficient (D_{ax})	3.8×10^{-2} m^2/s
Effective thermal conductivity (λ_L)	2.2×10^3 W/m/K

simulation runs are given in Table 4 and the results of the simulations are shown in Figure 8. The dots in the figure represent actual results of the simulation runs, while the line indicates the trend followed. As can be seen from the figure, the C_2H_4 product purity fell rapidly at high C_2H_4 product recovery for both the sorbents at constant productivity. High recovery was possible at low product purities, but it fell drastically at very high purity in the case of zeolite 4A. However, in the case of Ag^+–Amberlyst-35 resin sorbent, much higher C_2H_4 product recovery was possible compared to zeolite 4A at corresponding product purity and at the constant product throughput under consideration. Although, in general, the runs for Ag^+–resin show a slightly lower product throughput than that for zeolite 4A, comparison between runs 1 and 2 for Ag^+–resin and runs 6 and 7 for zeolite 4A in Table 4 is valid, since product throughputs are about the same for both. Hence, it can be concluded that equilibrium separation by π-complexation adsorbents such as Ag^+–Amberlyst-35 gives better performance than kinetic separation using zeolite 4A. Moreover, both curves in Figure 8 could be raised by further lowering the product throughput. Although product purities in excess of 99.9% were possible for the Ag^+–resin at recoveries lower than 10%, the product throughput dropped further. Hence these data could not be shown in this figure. The monolayer $AgNO_3/SiO_2$ sorbent developed in our laboratory has selectivity for ethylene similar to that of Ag^+–resin and in addition has much higher diffusivities compared to the latter sorbent. Hence the disadvantage of having low product

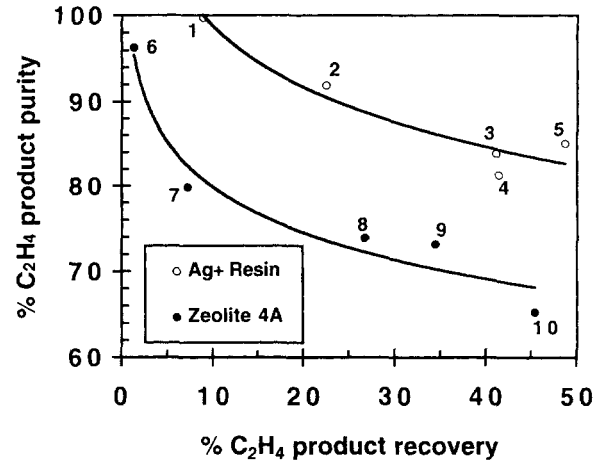

Figure 8. C_2H_4 product purity (%) vs. C_2H_4 product recovery (%) for PSA using zeolite 4A and Ag^+-exchanged Amberlyst-35 resin at average C_2H_4 product throughput = 1.1×10^{-4} kg of product/h/kg of adsorbent.

Feed temperature = 25°C. Inset figures refer to the number of the corresponding run shown in Table 4.

throughputs for Ag^+–resin can be overcome by using the $AgNO_3/SiO_2$ sorbent with negligible diffusion limitation.

Simulation studies were also carried out for Bergbau-Forschung CMS. It can be seen from the C_2H_4/C_2H_6 isotherms in Figure 6 that C_2H_6 was excluded almost completely from the pores, whereas C_2H_4 is not. A study of the C_2H_4 uptake curves for CMS showed that the uptake was very slow, requiring more than 1 h to reach 80–90% of uptake for C_2H_4, even at a high temperature of 100°C. Simulation runs were carried out at 100°C with a step time ranging from 4,000 to 8,000 s. Since the cycle time was high, the product throughput was very low compared to that of zeolite 4A and Ag^+–Amberlyst-35. Also, since the working capacity of the CMS adsorbent for C_2H_4 was quite small compared to that possessed by the other two adsorbents, there was a large restriction on the feed throughput and on the allowable purge-to-feed ratio. The results of PSA simulations showed that although product purities over 90% were possible, the product

Table 4. PSA Operating Parameters for Comparison of Performances of Zeolite 4A and Ag^+-Exchanged Amberlyst-35 Resin for the Separation of C_2H_4 and C_2H_6*

Run No.	Step Time (s)	Time Const. t_s (s)	Interstit. Feed Vel. U_H (m/s)	Interstit. Purge Vel. U_P (m/s)	Desorp. Product (C_3H_6) % Purity	Desorp. Product C_3H_6 % Recovery	Desorp. Product (C_3H_6) Throughput (kg of Product/h/kg of Adsorbent)$\times10^3$
Ag^+ – Resin (Feed temperature = Initial temperature = 25°C)							
1	1,800	450	0.40	0.01	99.73	8.81	0.135
2	800	200	0.15	0.02	91.92	22.46	0.062
3	1,200	300	0.10	0.05	83.86	41.12	0.058
4	1,000	250	0.10	0.01	81.26	41.38	0.061
5	1,380	345	0.08	0.01	85.09	48.73	0.054
Zeolite 4A Sorbent (Feed temperature = Initial temperature = 25°C)							
6	80	15	1.30	0.15	96.33	1.32	0.109
7	480	120	0.10	0.03	79.83	7.18	0.032
8	80	15	0.30	0.10	73.91	26.71	0.292
9	120	30	0.10	0.08	73.19	34.50	0.160
10	300	80	0.05	0.03	65.29	45.33	0.116

*P_H = 1.0 atm; P_L = 0.1 atm.

recoveries would not exceed 5%. The low diffusivity of the olefin caused the feed to break through the bed even at interstitial velocities as low as 0.05 m/s, thus causing considerable loss of olefin in the feed product. Even at lower product purities, the recoveries did not improve much. Further, the maximum product throughput that could be achieved was of the order of 1.4×10^{-5} kg/h/kg sorbent, which is only 1% of that possible by zeolite 4A and Ag^{+}–resin. It was thus obvious that the performance of Bergbau-Forschung CMS as a sorbent for C_2H_4/C_2H_6 was very poor compared to the other sorbents despite having the property of excluding C_2H_6.

Propane/propylene separation

For the case of propane/propylene, the adsorbents that were considered for separation were zeolite 4A and monolayer $AgNO_3/SiO_2$. Zeolite 4A almost excludes propane from its pores, as can be seen from Figure 4, and hence makes it an excellent prospect for C_3H_6/C_3H_8 separation. The $AgNO_3/SiO_2$ adsorbent developed in our laboratory possesses a good selectivity, steep isotherm, and hence a large working capacity for C_3H_6 compared to that for C_3H_8. Thus this sorbent, which employs equilibrium separation due to π-complexation, is also a good candidate for this separation. The Bergbau-Forschung CMS adsorbent was found to exclude both C_3H_6 and C_3H_8 from its pores, and hence it was not considered for this olefin/paraffin system.

The PSA cycle used for C_3H_6/C_3H_8 separation was identical to that used for C_2H_4/C_2H_6 separation discussed earlier. In the case of zeolite 4A, separation was due to the difference in diffusion rate of the two species, and hence the cycle time had to be optimized. From a study of the uptake curves shown in Figure 5, it was decided to use step times ranging from 100 s to 800 s. As opposed to this, the $AgNO_3/SiO_2$ sorbent was found to have very fast uptake rates, and hence short step times of 60 to 400 s were used. The feed temperatures in the case of zeolite 4A and $AgNO_3/SiO_2$ were 100°C and 70°C, respectively.

The results of the PSA simulations are shown in Figure 9. The corresponding cycle conditions for the runs shown in the figure are summarized in Table 5. Since the product throughputs obtained for the two sorbents were quite different, the product recovery and purity could not be compared at the same product throughput, as was done in case of C_2H_4/C_2H_6 separation. Instead, the C_3H_6 product throughput of the two sorbents was compared at the same product purity of about 99%. As can be seen from Figure 9, the $AgNO_3/SiO_2$ sorbent gave almost five times the product throughput as was given by zeolite 4A. It should be noted that the main purpose of this work was to compare the performance of two types of sorbent under nearly identical cycle conditions rather than provide the optimal performance of each sorbent. The product recovery can be increased by further decreasing the product throughput or decreasing the product purity. For both sorbents, product recoveries in excess of 70% were possible when product purity was lowered to 95% at product throughput of the order of 1×10^{-3} kg of product/h/kg of adsorbent.

It was interesting to note the parabolic nature of product throughput vs. product recovery curve at constant product purity for $AgNO_3/SiO_2$. There appeared to be an optimal productivity at a particular recovery. For a PSA cycle, the aforementioned three performance variables are interrelated in a complex manner. The data points for $AgNO_3/SiO_2$ in

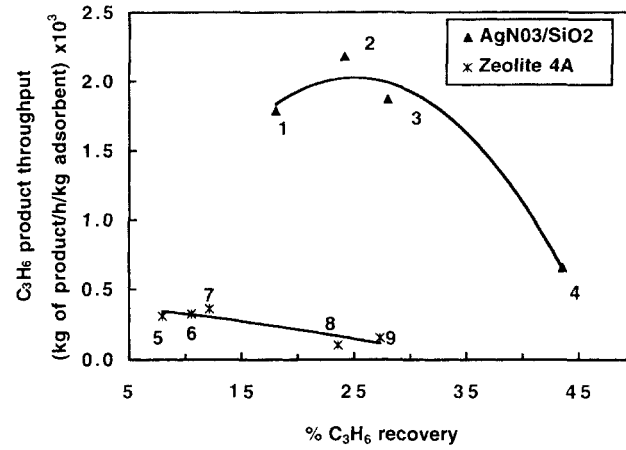

Figure 9. C_3H_6 product throughput vs. C_3H_6 % product recovery in the case of zeolite 4A and monolayer $AgNO_3/SiO_2$ at 99.1% C_3H_6 product purity.

Feed temperature for zeolite 4A and $AgNO_3/SiO_2$ sorbents is 100° and 70°C, respectively. Inset figures refer to the number of the corresponding run shown in Table 5.

Table 5. PSA Operating Parameters for Comparison of Performances of Zeolite 4A and Monolayer $AgNO_3/SiO_2$ for the Separation of C_3H_6 and C_3H_8*

Run No.	Step Time (s)	Time Const. t_s (s)	Interstit. Feed Vel. U_H (m/s)	Interstit. Purge Vel. U_P (m/s)	Desorp. Product (C_3H_6) % Purity	Desorp. Product C_3H_6 % Recovery	Desorp. Product (C_3H_6) Throughput (kg of Product/h/kg of Adsorbent)$\times10^3$
$AgNO_3/SiO_2$ Sorbent (Feed temperature = Initial temperature = 70°C)							
1	60	16	1.40	0.90	98.57	18.08	1.79
2	60	16	1.40	0.80	97.60	24.12	2.19
3	150	35	1.00	0.32	99.03	27.97	1.87
4	400	110	0.20	0.10	99.05	43.58	0.65
Zeolite 4A Sorbent (Feed temperature = Initial temperature = 100°C)							
5	100	30	0.80	0.13	99.94	7.95	0.31
6	400	110	0.70	0.05	99.10	10.54	0.36
7	400	110	0.60	0.05	99.01	12.16	0.40
8	800	240	0.08	0.045	99.97	23.59	0.10
9	600	150	0.10	0.065	99.98	27.29	0.15

*P_H = 1.0 atm; P_L = 0.1 atm.

Figure 9 at lower recovery values were obtained at short step times, whereas those at higher recovery values were those at long step times, as can be seen in Table 4. The capacity of the sorbent was utilized to a greater extent when step time was increased. Moreover, less of the olefin was wasted as a product of the feed step, and hence recovery was seen to improve with an increase in step time. Hence, as the step time was increased from a low value, there was initially a rise in productivity as well as product recovery. However, with further increase in step time, the number of cycles performed per hour decreased, thus resulting in decrease in product throughput. In addition, as the step time was increased, the less-adsorbed component, that is, C_3H_8, also diffused to a greater extent. This is more so for separation by $AgNO_3/SiO_2$ than by zeolite 4A because C_3H_8 has greater diffusivity with a higher temperature dependence than that of C_3H_6 for the former sorbent, as can be seen from Table 2. Hence, as per definition (Eq. 3), the product throughput decreased with higher step times, thus giving a parabolic curve.

Multiplicity of cyclic steady states

The transient C_3H_6 product purity vs. the cycle number was studied at adsorption pressure of 1 atm, desorption pressure of 0.1 atm, feed temperature of 70°C, step time of 210 s, time constant (t_s) of 50 s, and purge velocity of 0.186 m/s. The bed was initially saturated at 0.1 atm with a mixture of 5% C_3H_6 and 95% C_3H_8 at 70°C. The variation of product purity as the system approached cyclic steady state at different feed velocities is shown in Figure 10. A sudden jump of product purity from 80% to 98% was observed as purge velocity was increased from 0.80 m/s to 0.81 m/s. The transient product purity curves at intermediate feed velocity values showed a sigmoidal nature. It seemed as if the system tended toward an intermediate steady state (seemingly an unstable state), but then bifurcated to approach two different steady states. The product purity obtained at different feed velocities at the same purge velocity of 0.186 m/s is shown in Figure 11. All the other conditions were fixed at the values given earlier. For an initial temperature of 70°C, the product purity remained at 79.9% as feed velocity was increased from 0.72 m/s to 0.80 m/s (lower branch of Figure 11). Thereafter, at the feed velocity of 0.80 m/s and beyond, the product purity suddenly increased to 98.4%. At the same time, product recovery suddenly decreased from 41% to 28% as feed velocity was increased from 0.80 m/s to 0.81 m/s. In another set of simulations, keeping all the other parameters the same, the product purity was studied at different feed velocities with an initial temperature of 120°C. In this case, the product purity and product recovery remained at 79.9% and 41%, respectively, until feed velocity of 0.75 m/s. Beyond this value, the product purity jumped to 98.8% and the product recovery decreased to 28% (upper branch of Figure 11). Thus, for the range of feed velocities from 0.75 m/s to 0.80 m/s, two different cyclic steady states were observed with respect to initial temperature of the PSA bed. Kikkinides et al. (1995) had seen a similar behavior of multiplicity for the system of $H_2S/CO_2/CH_4$ on 5A zeolite. In their case, multiplicity of steady states was observed with respect to different initial concentrations of the sorbates. However, in the present work, simulations carried out with different initial concentrations did not display multiplicity of periodic steady states.

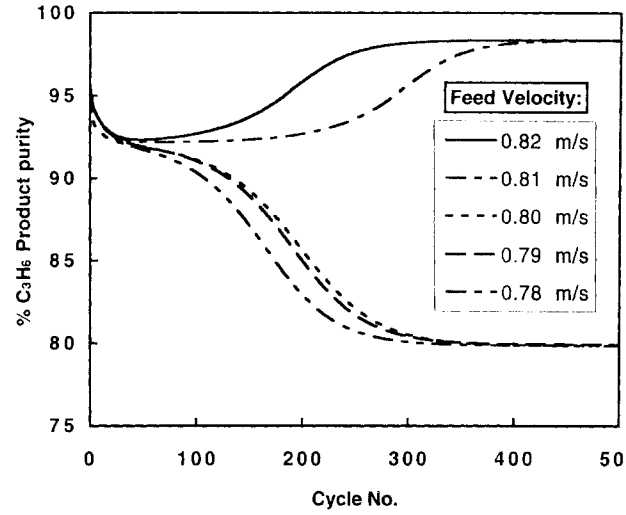

Figure 10. Transient behavior of C_3H_6 concentration in the desorption product from step 4 as system approaches cyclic steady state at different feed velocities starting from a bed saturated with 5% C_3H_6 and 95% C_3H_8 at 0.1 atm in the case of $AgNO_3/SiO_2$ sorbent.

P_H = 1.0 atm; P_L = 0.1 atm; step time = 210 s; purge velocity = 0.186 cm/s; feed temperature = initial temperature = 70°C.

A similar type of behavior was observed with change in purge velocity. As before, when the initial temperatures of the bed were altered from 70°C to 120°C, the system displayed multiple steady states for a range of purge velocities. Figure 12 displays the transient product purity profiles as the system approaches cyclic steady state for adsorption pressure of 1 atm, desorption pressure of 0.1 atm, feed temperature of 70°C, step time of 210 s, time constant (t_s) of 50 s, feed velocity of 0.80 m/s, and purge velocity ranging from 0.18 m/s to

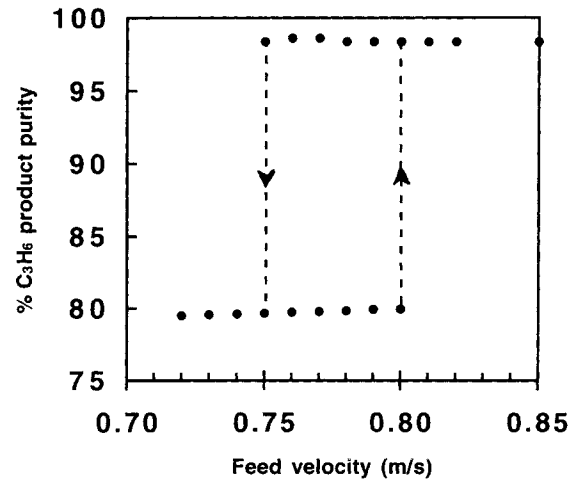

Figure 11. Multiplicity in PSA cyclic steady states with $AgNO_3/SiO_2$.

Effect of interstitial feed velocity, U_H, on the C_3H_6 concentration in the desorption (step 4) product. The lower branch started with initial temperature of 70°C, while the upper branch started with that of 120°C. P_H = 1.0 atm; P_L = 0.1 atm; step time = 210 s; purge velocity = 0.186 cm/s; feed temperature = 70°C.

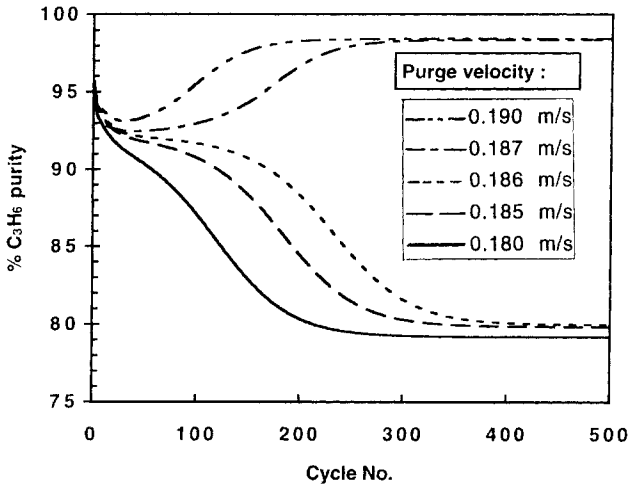

Figure 12. Transient behavior of C_3H_6 concentration in the desorption product from step 4 as system approaches cyclic steady state at different purge velocities starting from a bed saturated with 5% C_3H_6 and 95% C_3H_8 at 0.1 atm in the case of $AgNO_3/SiO_2$ sorbent.

Feed temperature = initial temperature = 70°C. P_H = 1.0 atm; P_L = 0.1 atm; step time = 210 s; feed velocity = 0.80 cm/s.

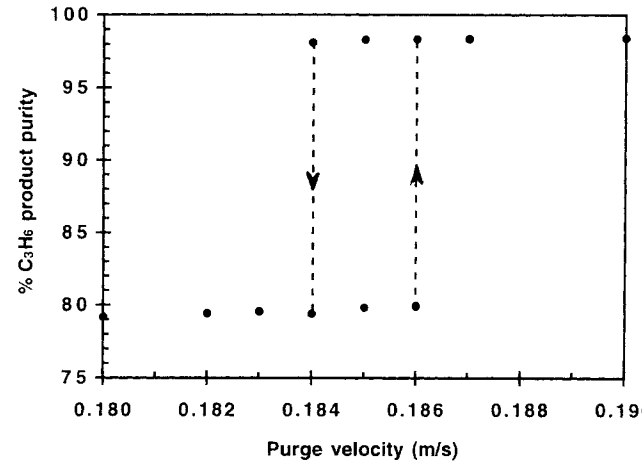

Figure 13. Multiplicity in PSA cyclic steady states with $AgNO_3/SiO_2$.

Effect of interstitial purge velocity, U_P, on the C_3H_6 concentration in the desorption (step 4) product. The lower branch started with initial temperature of 70°C while the upper branch started with that of 120°C. P_H = 1.0 atm; P_L = 0.1 atm; step time = 210 s; feed velocity = 0.80 cm/s; feed temperature = 70°C.

0.19 m/s. The approach to a middle unstable state and then its bifurcation to upper and lower stable steady states seen in Figure 12 was similar to that in Figure 10. The effect of the interstitial purge velocity on the C_3H_6 product concentration starting from two different initial temperatures is shown in Figure 13. The lower branch in the figure represents the product purities obtained when the bed was started with an initial temperature of 70°C. As the purge velocity was increased from 0.186 m/s to 0.187 m/s, the product purity suddenly increased to 98.4% from 80%. The upper branch was obtained by starting with an initial temperature of 120°C, and a similar jump was seen at 0.184 m/s. Thus for the small range of purge velocities between 0.184 m/s and 0.186 m/s, multiple steady states were observed with respect to the initial temperature of the bed. A further study of the effect of initial temperature on the product-purity dependence of feed and purge velocity in the region of multiplicity revealed that all simulations carried out at initial temperatures below 106°C followed the behavior observed for the initial temperature of 70°C, whereas all initial temperatures above 107°C gave the behavior observed for that of 120°C. A detailed discussion of the phenomenon of multiplicity of cyclic steady states and their probable causes will be the subject of a further study.

Conclusions

The performance of three types of adsorbents, namely, those involving kinetic separation, exclusion of one of the components, and equilibrium separation, was compared for C_2H_4/C_2H_6 and C_3H_6/C_3H_8 systems using PSA simulations of a four-step cycle involving cocurrent purge with the strongly adsorbed species, that is, olefin. In case of the ethane/ethylene system, equilibrium separation using Ag^+-exchanged Amberlyst-35 sorbent was found to be superior compared to the kinetic separation carried out by zeolite 4A by a study of the product purity vs. recovery curve at constant product throughput. The performance of carbon molecular sieve, which was found to exclude C_2H_6 from the pores, was found to be poor compared to both zeolite 4A and Ag^+-exchanged resin, mainly because of its slow uptake rates. For the propane/propylene separation, equilibrium separation by monolayer $AgNO_3/SiO_2$ sorbent was found to be superior to the kinetic separation by zeolite 4A. In this case comparison was performed by comparing the product throughputs obtained using the two sorbents at a fixed C_3H_6 product purity of 99.1%. For C_3H_6/C_3H_8 separation on $AgNO_3/SiO_2$ sorbent, multiplicity of cyclic steady states was observed within certain ranges of feed and purge velocities. Within these ranges, simulation of the PSA starting from two different initial conditions while keeping the same operating conditions yielded two different stable cyclic steady states.

Spreading of monolayer $AgNO_3$ on varius substrates can also be accomplished by the incipient wetness technique. Details will be published shortly.

Acknowledgment

This work was supported by the NSF under Grant CTS-9520328. We are grateful to Professor Don Paul of Texas who first suggested the problem of olefin-paraffin separations to RTY.

Notation

c_p = specific heat, kcal/g/K
E_{act} = diffusional energy of activation, kcal/mmol
ΔH = heat of adsorption, kcal/mol
L = total length of the adsorption bed, m
P = total pressure, bar
$\bar{q}$ = volume-averaged adsorbed amount, mmol/g
R = gas constant, kcal/mmol/K
R_p = radius of particle, m
t = time, s
T = temperature, K
u = interstitial gas velocity, m/s
y = mole fraction of the components in the gas phase
z = axial coordinate in the bed, m
ϵ = void fraction of the packing
ϵ_t = bed void fraction including macropores in particles

ρ_b = bed density, kg/m^3
ρ_g = gas phase density, kg/m^3
τ = time duration of process step, s

Subscripts

fin = final condition
g = gas phase
H = corresponding to the feed step
P = corresponding to the purge step
i = species i
ini = initial condition
j,k = gas phase component index
L = low pressure corresponding to purge step
s = solid phase

Literature Cited

Aris, R., "On Stability Criteria of Chemical Reaction Engineering," *Chem. Eng. Sci.*, **24**, 149 (1969).

Barett, E. P., L. S. Joyner, and P. P. Halenda, "Determination of Pore Volume and Area Distributions in Porous Substances. I. Computations from Nitrogen Isotherms," *J. Amer. Chem. Soc.*, **73**, 373 (1951).

Blytas, G. C., "Separation of Unsaturates by Complexing with Non-Aqueous Solutions of Cuprous Salts," *Separation and Purification Technology*, Chap. 2, N. N. Li and J. M. Clao, eds., Dekker, New York (1992).

Carnahan, B., H. A. Luther, and J. O. Wilkes, *Applied Numerical Methods*, Wiley, New York (1969).

Cen, P. L., "Simultaneous Physical and Chemical Adsorption of Ethylene and Cu(I) NaY Zeolite," *Fundamentals of Adsorption*, A. B. Mersmann and S. E. Scholl, eds., Engineering Foundation, New York, p.191 (1991).

Cen, P. L., and R. T. Yang, "Separation of Binary Gas Mixture into Two High-Purity Products by a New Pressure Swing Adsorption Cycle," *Sep. Sci. Technol.*, **21**, 845 (1986).

Chen, Y. D., R. T. Yang, and R. Uawithya, "Diffusion of Oxygen, Nitrogen, and Their Mixtures in Carbon Molecular Sieve," *AIChE J.*, **40**, 577 (1994).

Chen, J. P., and R. T. Yang, "Molecular Orbital Study of Selective Adsorption of Simple Hydrocarbons on Ag^+ and Cu^+ Exchanged Resins and Halides," *Langmuir*, **11**, 3450 (1995).

Chen, N., and R. T. Yang, "*Ab Initio* Molecular Orbital Study of Adsorption of O_2, N_2, and C_2H_4 on Ag-Zeolite and Ag Halides," *Ind. Eng. Chem. Res.*, **35**, 4020 (1996).

Cheng, L. S., and R. T. Yang, "Monolayer Cuprous Chloride Dispersed on Pillared Clays Olefin-Paraffin Separations by π-Complexation," *Adsorption*, **1**, 61 (1995).

Cotton, F. A., and G. Wilkinson, *Advanced Inorganic Chemistry*, 2nd ed., Chaps. 25 and 28, Interscience, New York (1966).

Croft, D. T., and M. D. LeVan, "Periodic States of Adsorption Cycles: I. Direct Determination and Stability," *Chem. Eng. Sci.*, **49**, 1821 (1994a).

Croft, D. T., and M. D. LeVan, "Periodic States of Adsorption Cycles: II. Solution Spaces and Multiplicity," *Chem. Eng. Sci.*, **49**, 1831 (1994b).

Eldridge, R. B., "Olefin/Paraffin Separation Technology: A Review," *Ind. Eng. Chem. Res.*, **32**, 2208 (1993).

Gavalas, G. R., "On the Steady States of Distributed Parameter Systems with Chemical Reactions, Heat and Mass Transfer," *Chem. Eng. Sci.*, **21**, 477 (1966).

Ghosh, T. K., H. D. Lin, and A. L. Hines, "Hybrid Adsorption-Distillation Process for Separating Propane and Propylene," *Ind. Eng. Chem. Res.*, **32**, 2390 (1993).

Gilliland, E. R., "Concentration of Olefins," U.S. Patent No. 2,369,559 (1945).

Gilliland, E. R., H. L. Bliss, and C. E. Kip, "Reactions of Olefins with Solid Cuprous Halide," *J. Amer. Chem. Soc.*, **63**, 2088 (1941).

Hirai, H., S. Hara, and M. Komiyama, "Polystyrene-Supported Aluminum Silver Chloride as Selective Ethylene Adsorbent," *Angew. Makromol. Chem.*, **130**, 207 (1985a).

Hirai, H., K. Kurima, K. Wada, and M. Komiyama, "Selective Ethylene Adsorbents Composed of Cu(I)Cl and Polystyrene Resins Having Amino Groups," *Chem. Lett. (Jpn)*, 1513 (1985b).

Ho, W. S., G. Doyle, D. W. Savage, and R. L. Pruett, "Olefin Separations via Complexation with Cuprous Diketonate," *Ind. Eng. Chem. Res.*, **27**, 334 (1988).

Iooss, G., and D. D. Joseph, *Elementary Stability and Bifurcation Theory*, Springer-Verlag, New York (1980).

Jarvelin, H., and H. R. Fair, "Adsorptive Separation of Propylene-Propane Mixtures," *Ind. Eng. Chem. Res.*, **32**, 2201 (1993).

Jensen, K. F., and W. H. Ray, "The Bifurcation Behavior of Tubular Reactors," *Chem. Eng. Sci.*, **37**, 199 (1982).

Kärger, J., and D. M. Ruthven, *Diffusion in Zeolites and Other Microporous Solids*, Wiley, New York (1992).

Keller, G. E., A. E. Marcinkowsky, S. K. Verma, and K. D. Wiliamson, "Olefin Recovery and Purification via Silver Complexation," *Separation and Purification Technology*, N. N. Li, and J. M. Calo, eds., Dekker, New York, p. 59 (1992).

Khinast, J., and D. Luss, "Mapping Regions with Different Bifurcation Diagrams of a Reverse-Flow Reactor," *AIChE J.*, **43**, 2034 (1997).

Kikkinides, E. S., R. T. Yang, and S. H. Cho, "Concentration and Recovery of CO_2 from Flue Gas by Pressure Swing Adsorption," *Ind. Eng. Chem. Res.*, **32**, 2714 (1993).

Kikkinides, E. S., V. I. Sikavitsas, and R. T. Yang, "Natural Gas Desulfurization by Adsorption: Feasibility and Multiplicity of Cyclic Steady States," *Ind. Eng. Chem. Res.*, **34**, 255 (1995).

King, C. J., "Separation Processes Based on Reversible Chemical Complexation," *Handbook of Separation Process Technology*, Chap. 15, R. W. Rousseau, ed., Wiley, New York (1987).

Kumar, R., T. C. Golden, T. R. White, and A. Rokicki, "Novel Adsorption Distillation Hybrid Scheme for Propane/Propylene Separation," *Sep. Sci. Technol.*, **27**, 2157 (1992).

Kumar, R., W. C. Kratz, D. E. Guro, and T. C. Golden, "A New Process for the Production of High Purity Carbon Monoxide and Hydrogen," Int. Symp. on Separation Technology, Univ. of Antwerp, Belgium (1993).

Kulvaranon, S. M., M. E. Findley, and A. I. Liapsis, "Increased Separation by Variable-Temperature Stepwise Desorption in Multicomponent Adsorption Processes," *Ind. Eng. Chem. Res.*, **29**, 106 (1990).

Long, R. B., "Separation of Unsaturates by Complexing with Solid Copper Salts," *Recent Developments in Separation Science*, Vol. 1, N. N. Li, ed., CRC Press, Cleveland, OH, p. 35 (1972).

Luss, D., and N. R. Amundson, "Uniqueness of the Steady State Solutions for Chemical Reaction Occurring in a Catalyst Particle or in a Tubular Reactor with Axial Diffusion," *Chem. Eng. Sci.*, **22**, 253 (1967).

Padin, J., and R. T. Yang, "Tailoring New Adsorbents Based on π-Complexation: Cation and Substrate Effects on Selective Acetylene Adsorption," *Ind. Eng. Chem. Res.*, **36**, 4224 (1997).

Quinn, H. W., "Hydrocarbon Separations with Silver (I) Systems," *Progress in Separation and Purification*, Vol. 4, E. S. Perry, ed., Interscience, New York, p. 133 (1971).

Ramachandran, R., and L. Dao, "Separation of Hydrocarbon Mixtures," European Patent Application 572,239 (1993) (cited in *Zeolites*, **15**, 384 (1995)).

Sircar, S., and J. W. Zondlo, "Fractionation of Air by Adsorption," U.S. Patent No. 4,013,429 (1977).

Sun, L. M., P. Le Quere, and M. D. Le Van, "Numerical Simulation of Diffusion-Limited PSA Process Models by Finite Difference Methods," *Chem. Eng. Sci.*, **51**, 5341 (1996).

Wu, Z., S.-S. Han, S.-H. Cho, J.-N. Kim, K.-T. Chue, and R. T. Yang, "Modification of Resin-Type Adsorbents for Ethane-Ethylene Separation," *Ind. Eng. Chem. Res.*, **36**, 2749 (1997).

Xie, Y.-C., and Y.-Q. Tang, "Spontaneous Monolayer Dispersion of Oxides and Salts onto Surfaces of Supports: Applications to Heterogeneous Catalysis," *Adv. Catal.*, **37**, 1 (1990).

Yang, R. T., *Gas Separation by Adsorption Processes*, Butterworth, Boston (1987).

Yang, R. T., and E. S. Kikkinides, "New Sorbents for Olefin/Paraffin Separations by Adsorption via π-Complexation," *AIChE J.*, **41**, 509 (1995).

Yang, R. T., and R. Foldes, "New Adsorbents Based on Principles of Chemical Complexation: Monolayer-Dispersed Nickel (II) for Acetylene Separation by π-Complexation," *Ind. Eng. Chem. Res.*, **35**, 1006 (1996).

Manuscript received Nov. 5, 1997, and revision received Feb. 9, 1998.